CFD study of PM10 dispersion in a sports stadium using a mesh based on a geometry obtained from a 3-D cloud of laser points

Hector Amino[1,2], Cédric Flageul[3], Bertrand Carissimo[2], Martin Ferrand[1,2]

[1]EDF R&D, MFEE, Chatou France
[2]CEREA (Ecole des Ponts ParisTech - EDF R&D)
[3]PPRIME Institute, Curiosity Group, Université de Poitiers, CNRS

June 11th, 2024

Context and motivation

Context

- **Indoor air quality** and **thermal comfort** $\rightarrow$ important stakes in large structures such as sport facilities
- Such elements are dependent on the heating, ventilation, and air conditioning systems (HVAC)
- Numerical simulations can provide insightful data to optimize/design HVAC

Context and motivation

Context

- **Indoor air quality** and **thermal comfort** → important stakes in large structures such as sport facilities
- Such elements are dependent on the heating, ventilation, and air conditioning systems (HVAC)
- Numerical simulations can provide insightful data to optimize/design HVAC

Motivation

For large sports facilities :

- Computational Fluid dynamics can provide useful/complementary local data
  but ...
- CFD prediction accuracy for complex thermo-aeraulic systems ?
- Reproduction of such detailed geometry ?

Context and motivation

Context

- **Indoor air quality** and **thermal comfort** → important stakes in large structures such as sport facilities
- Such elements are dependent on the heating, ventilation, and air conditioning systems (HVAC)
- Numerical simulations can provide insightful data to optimize/design HVAC

Motivation

For large sports facilities :

- Computational Fluid dynamics can provide useful/complementary local data
  but ...
- CFD prediction accuracy for complex thermo-aeraulic systems ?
- Reproduction of such detailed geometry ?

Proposition

One possible methodology for complex geometries CFD simulation using a high fidelity mesh based on 3D cloud of points

Methodology

Pierre de Coubertin stadium

Used for the Paralympic and Olympic Games

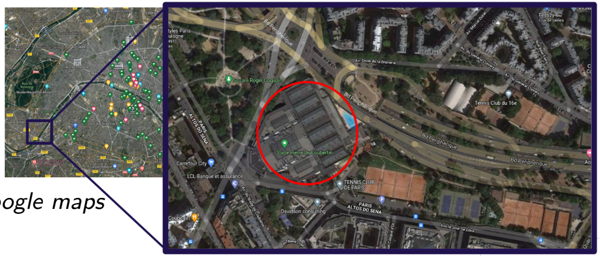

© *Google maps*

Around **4.5 k** seats

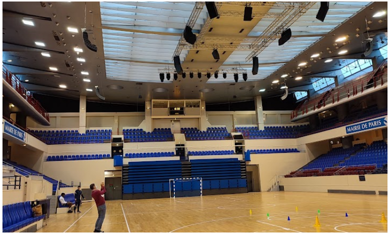

Methodology

Test case introduction

Reproduction using CFD of Particle Matter (PM10) during a handball game within the enclosed stadium

- Experimental campaign done by different laboratories during summer 2021 (*CSTB, LISA, LCPP, CEREA*)
- Local peak of PM10 concentration C_{PM10} caused by fireworks **in** and **outside** the stadium
- Use of the open source CFD software code_saturne
- Extension of the validation of a novel indoor air flow algorithm [Amino, H. Development of a CFD time scheme for indoor airflow applications, PhD, 2022]

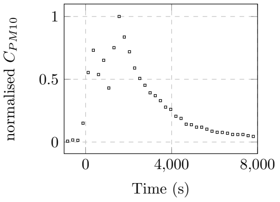

PM10 concentration measured over time (normalised values)

Difficulties

- Very detailed system
- Lack of information regarding the stadium heterogeneous fields

Fireworks outside the stadium

PM10 Sensor location (CSTB, LISA, LCPP, CEREA)

Mesh generation strategy

Presentation of 3D cloud of points based mesh : main steps

1. **Cloud of points generation and pre-processing**
   - Acquisition using a 3-D laser scanner
   - Parasite points cleaning
   - Rotation and translation into the the reference axis

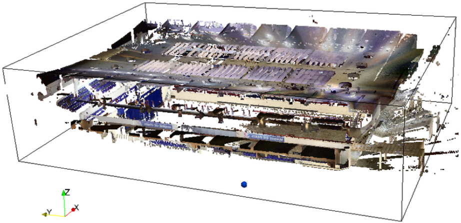

Stadium cloud of points [Lefranc Y., 2021]

Cloud of points inside visualization

Mesh generation strategy

Presentation of 3D cloud of points based mesh : main steps

1. Cloud of points generation and pre-processing
   - Acquisition using a 3-D laser scanner
   - Parasite points cleaning
   - Rotation and translation into the the reference axis
2. **Fluid volume definition**
   - Homogeneous box domain definition incorporating the cloud of points
   - Transport of the porosity $\Pi \in [0, 1]$ with source terms defined at the scanner locations

$$\frac{\partial \Pi}{\partial t} + \mathrm{div}(\Pi \underline{e}_r) - \mathrm{div}(\underline{e}_r) = 0$$

   - Fluid volume if porosity $\geq$ threshold (variable in space)

Porosity thresholds used to create the mesh

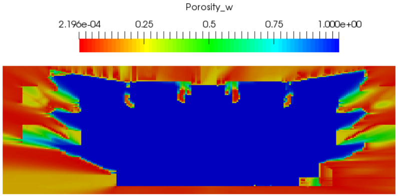

Porosity field for a threshold of 2.2e-4 : fake fluid cells

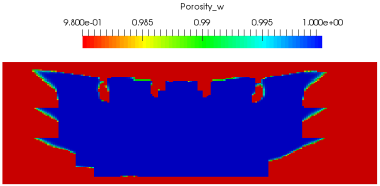

Porosity field for a threshold of 0.98 : lack of details

$\leftarrow$ compromise !

Mesh generation strategy

Presentation of 3D cloud of points based mesh : main steps

1. Cloud of points generation and pre-processing
   - Acquisition using a 3-D laser scanner
   - Parasite points cleaning
   - Rotation and translation into the the reference axis
2. Fluid volume definition
   - Homogeneous box domain definition incorporating the cloud of points
   - Transport of the porosity Π with source terms defined at the scanner locations

$$\frac{\partial \Pi}{\partial t} + \text{div}(\Pi \underline{e}_r) - \text{div}(\underline{e}_r) = 0$$

   - Fluid volume if porosity $\geq$ **threshold** (variable in space)
3. **Boundary zones definition**

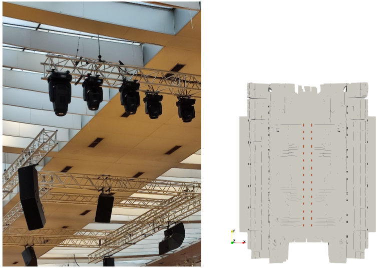

(Left) Illustration of the extraction vents. (Right) Corresponding zones.

Inside visualization of the outlets zones (in red)

Mesh used for simulations

Final mesh composed of 2.4 10^6 hexahedral cells ($\Delta x = \Delta y = \Delta z = 0.2$m)

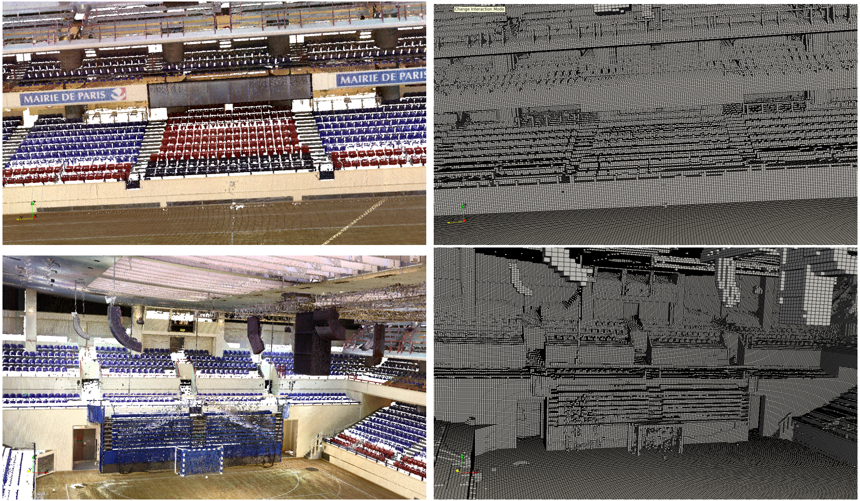

Mesh used for simulations

Final mesh composed of 2.4 10^6 hexahedral cells ($\Delta x = \Delta y = \Delta z = 0.2$m)

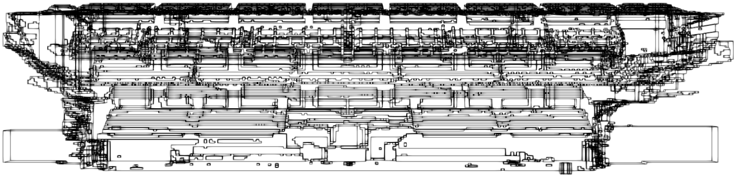

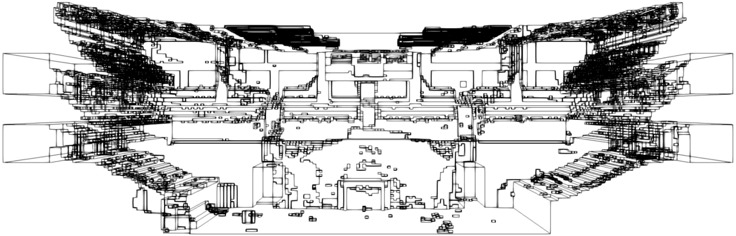

Different views of the mesh retained for the simulations

Numerical choices

Indoor airflow time scheme [Amino et. al., IJNMF, 2022]

- Navier–Stokes equations
- Implemented in code_saturne (F.V method)
- Prediction correction sub-iterative scheme
- Theta scheme ($\theta = 1$: Euler implicit, $\theta = 1/2$: Crank Nicolson)
- Able to predict incompressible and compressible flow
  - Account for the total pressure variation
  - Total energy conservation
- Validation in the indoor flow frawework made [Amino H., Flageul C., Tiselj, I., Benhamadouche S., Carissimo, B., Ferrand M., 2022. A time-staggered second order conservative time scheme for variable density flow, IJNMF]

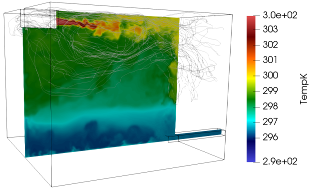

Validation example : snapshot of a hot ventilation jet

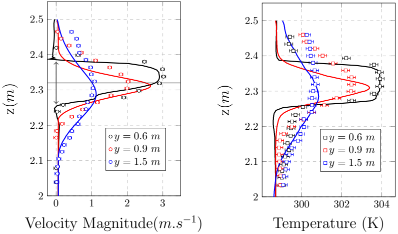

Velocity and temperature vertical profiles for different axial distances

Numerical choices

Simulation setup

- Isothermal ventilation
- $Q_{in} = 60\ 10^3 \mathrm{m}^3.\mathrm{h}^{-1}$ $(\approx 3 \times \Omega_{tot}/h)$
- $k - \varepsilon$ model for turbulence
- Transient inlet condition :
  - $t \leq 1550$ s (peak) : inlet of PM10 and air
  - else : inlet of pure air

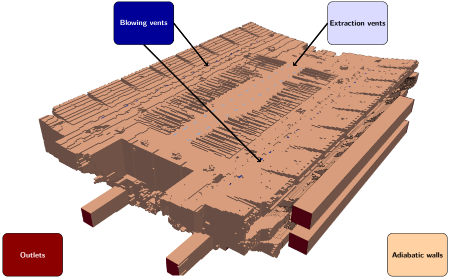

Boundary conditions zones imposed for this simulation.

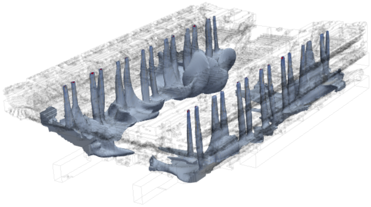

Illustration of the PM10 injection

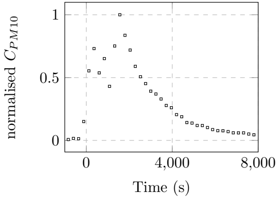

PM10 concentration measured over time.

Results

CFD results compared to the experimental data and a simplified 0D model (homogeneous mixture)

- Evolution shape agreement
- Larger error for the simplified model

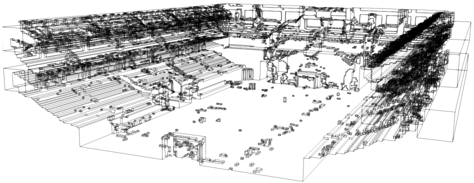

Local PM10 concentration over time

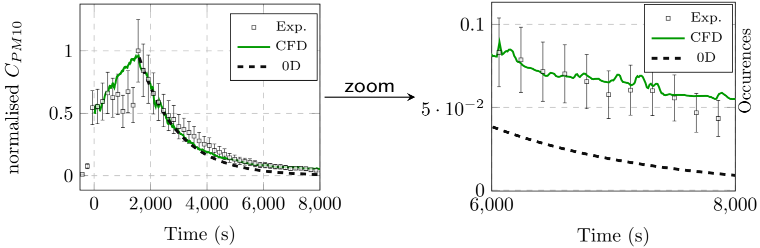

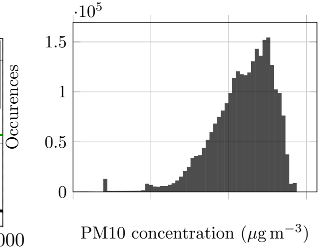

PM10 concentration histogram at 1600 s

Results

CFD also provides 3D insights of the indoor air flow such as :

the local dynamic field

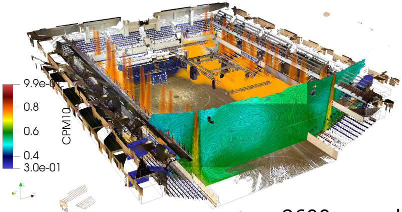

the local residence time

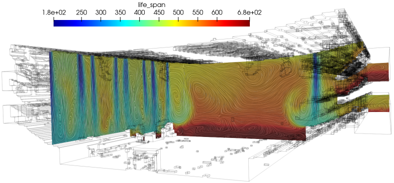

$t = 3600$ s : volumes whose residence time is above 1400 s

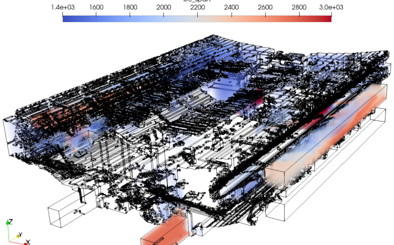

Conclusion

- A methodology leading to **high fidelity** meshes is presented and applied to a stadium CFD study
- Numerical results were in agreement with the experimental data
- Such validation result emphasises the methodology potential in the CFD simulation framework
- Extended to external simulations

Further method improvements :

- Use of more advanced immersed boundary methods e.g. :

  [Narvaez, et al., 2023, Automatic Solid Reconstruction from 3-D Points Set for Flow Simulation via an Immersed Boundary Method. FVCA]
- Boundary zones identification/automatization

Conclusion

Thank you for your attention.

hector.galante-amino@edf.fr

Acknowledgements :
EDF R&D and CEREA : Yannick Lefranc, Aurélien Facheux for the 3D cloud of points measurements
CSTB, LISA, LCPP, CEREA for experimental data and discussions
Mairie de Paris for the visits and informations regarding the stadium
Financial support by ANRT through an EDF-CIFRE contract

Simulation time

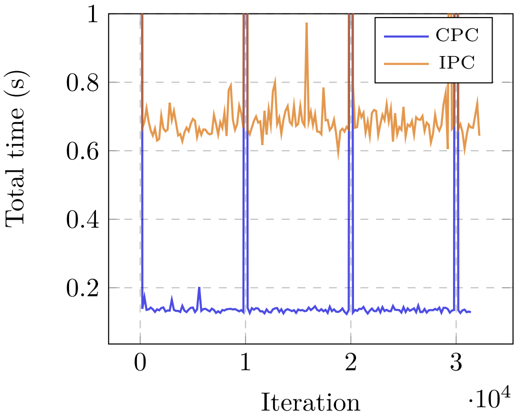

Coubertin simulation (100 physical seconds, 2M cells, 175 procs) isothermal problem

Solver	IPC time (s)	CPC time (s)
Temperature	1.17	3.3483
Velocity	10.4	11.8
k	2.38	2.84
ε	2.6	3.0
Pressure	2143.5 (2096.2)	195.1
Total time	2206.4	260.4

Scheme equations

Navier–Stokes compressible equations :

$$\frac{\partial \rho}{\partial t} + \text{div}\,(\rho \underline{u}) = 0,$$

$$\frac{\partial \rho \underline{u}}{\partial t} + \underline{\text{div}}\,(\underline{u} \otimes \rho \underline{u}) = -\underline{\nabla} p + \underline{\text{div}}\left(\underline{\underline{\tau}}\right) + \overbrace{\underline{f}}^{\rho \underline{g}},$$

$$\frac{\partial (\rho e)}{\partial t} + \text{div}\,(e \rho \underline{u}) = -p\,\text{div}\,(\underline{u}) + \underline{\underline{\tau}} : \underline{\underline{\nabla u}} + \text{div}\,(\lambda \underline{\nabla} T),$$

$$\frac{\partial (\rho Y)}{\partial t} + \text{div}\,(Y \rho \underline{u}) = \text{div}\,(K \underline{\nabla} Y),$$

$$T = \mathcal{T}(\rho, e) = \frac{\gamma - 1}{R_a}\, e$$

$$p = \mathcal{P}(\rho, e) = \rho R_a T.$$

Set of equations chosen to be discretised

Density variation

- Buoyant effects

Local Thermodynamic pressure variation

Proposition : compressible pressure correction (CPC) scheme

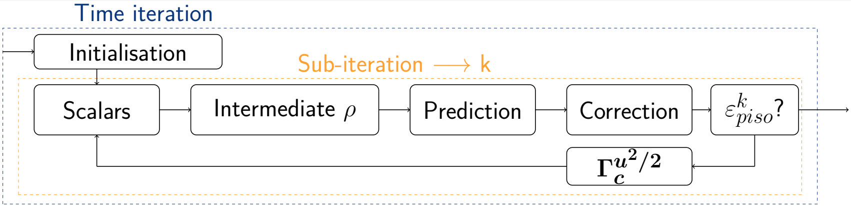

Features

- Variable time convergence order
- Total energy conservation
- ρ dependence on T
- EOS linearisation
- ρ dependence on p

Proposition : compressible pressure correction (CPC) scheme

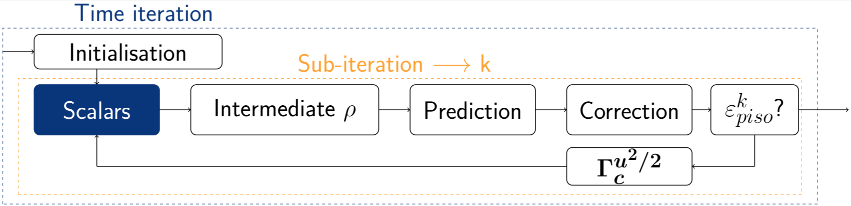

Features

- Variable time convergence order
- Total energy conservation
- ρ dependence on T
- EOS linearisation
- ρ dependence on p

Internal energy equation solved in $[n; n+1, k] \longrightarrow e_c^{n+1,k}$

$$\frac{\rho_c^{n+1,k-1} e_c^{n+1,k} - \rho_c^{n,k-1} e_c^n}{\Delta t} + \mathrm{Div}_c\left(\left\langle \Theta\left(e^n,\ e^{n+1,k}\right)\right\rangle_f \underline{q}_f \Big|_n^{n+1,k-1}\right) = \mu \overbrace{(S_c^2)^{n+\theta,k-1}}^{\text{Dissipation function}} + \Gamma_c^{u^2/2}\Big|_n^{n+1,k-1}$$

$$+ \mathrm{Lapl}_c\left(\lambda, \Theta\left(T^n,\ T^{n+1,k}\right)\right) - \mathrm{Div}_c\left(\left\langle\Theta\left(p^n,\ p^{n+1,k-1}\right)\underline{u}^{n+\theta,k-1}\right\rangle_f\right) + \underline{u}_c^{n+\theta,k-1}\cdot \underline{\nabla}_c\, p\Big|_{n-1+\theta}^{n+\theta,k-1}$$

$\Gamma^{u^2/2}$: corrective source term $\longrightarrow$ kinetic energy dissipation, derived from its discrete equation [Amino et al., 2022] adapted from Herbin et al., 2020

$$T_c^{n+1,k} = e_c^{n+1,k} c_v^{-1}$$

[Amino et al., A time-staggered second order conservative time scheme for variable density flow. IJNMF, 2022]
[Herbin, Zaza, Latché, A cell-centered pressure-correction scheme for the compressible Euler equations, IMA Journal of Numerical Analysis, 40, 2020]

Proposition : compressible pressure correction (CPC) scheme

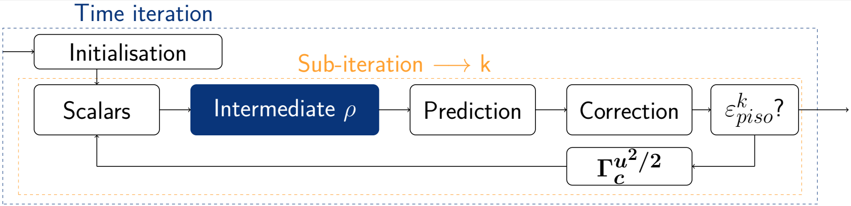

Features

- Variable time convergence order
- Total energy conservation
- ρ dependence on T
- EOS linearisation
- ρ dependence on p

Predicted density $\longrightarrow \widetilde{\rho}^k$

$$\widetilde{\rho}^k = \frac{p^{n+1,k-1}}{R_a T^{n+1,k}}$$

Proposition : compressible pressure correction (CPC) scheme

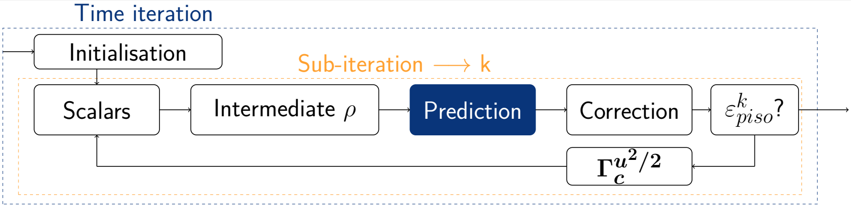

Features

- Variable time convergence order
- Total energy conservation
- ρ dependence on T
- EOS linearisation
- ρ dependence on p

Momentum equation solved between $[n-1+\theta; n+\theta, k] \longrightarrow \underline{\widetilde{u}}^k$

$$
\frac{\Theta\left(\rho_c^n,\, \rho_c^{n+1,k-1}\right)\underline{\widetilde{u}}_c^k - \Theta\left(\rho_c^{n-1},\, \rho_c^{n,k-1}\right)\underline{u}_c^{n-1+\theta}}{\Delta t} + \mathrm{Div}_c\left(\left\langle \Theta\left(\underline{u}^{n-1+\theta},\, \underline{\widetilde{u}}^k\right)\right\rangle_f \otimes \underline{q}_f\Big|_{n-1+\theta}^{n+\theta,k-1}\right)
$$
$$
= -\underline{\mathrm{Grad}}_c\left(\left\langle p\big|_{n-1+\theta}^{n+\theta,k-1}\right\rangle_f\right) + \mathrm{Div}_c\left(\left\langle \Theta\left(\underline{\underline{\tau}}^n,\, \underline{\underline{\tau}}^k\right)\right\rangle_f\right) + \underline{f}_c\big|_{n-1+\theta}^{n+\theta,k-1}.
$$

$\underline{\underline{\tau}} = \mu\left(\underline{\underline{\nabla}}\,\underline{u} + \underline{\underline{\nabla}}\,\underline{u}^T\right) - \frac{2}{3}\mu\mathrm{div}\left(\underline{u}\right)\underline{\underline{I}}$ (shear stress tensor)

Proposition : compressible pressure correction (CPC) scheme

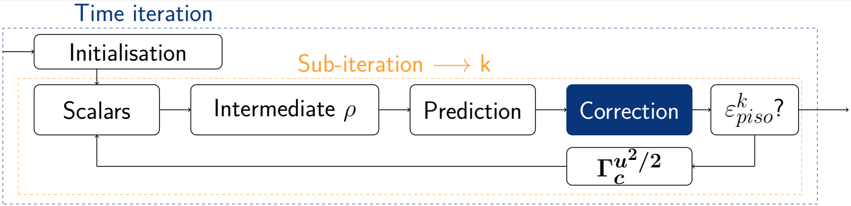

Features

- Variable time convergence order
- Total energy conservation
- ρ dependence on T
- EOS linearisation
- ρ dependence on p

Mass and simplified momentum equations solved between $[n; n+1, k]$

$$\begin{cases} \dfrac{\Theta\left(\rho_c^n,\, \rho_c^{n+1,k}\right) \underline{u}_c^{n+\theta,k} - \Theta\left(\rho_c^n,\, \rho_c^{n+1,k-1}\right) \underline{\widetilde{u}}_c^{k}}{\Delta t} + \underline{\nabla}_c \phi^k = 0, \\[2ex] \mathrm{Div}_c\left(\underline{q}_f \Big|_n^{n+1,k} \right) + \dfrac{\rho_c^{n+1,k} - \rho_c^n}{\Delta t} = 0, \qquad \phi_c^k = \Theta\left(p_c \Big|_{n-2+\theta}^{n-1+\theta},\, p_c^{n+1,k} \right) - p_c \Big|_{n-1+\theta}^{n+\theta,k-1}. \end{cases}$$

$$\rho_c^{n+1,k} = \widetilde{\rho}_c^{k} + \left(p_c^{n+1,k} - p_c^{n+1,k-1} \right) \left(\frac{\partial \rho}{\partial p} \right)_T \left(p_c^{n+1,k-1},\, T_c^{n+1,k} \right)$$

Proposition : compressible pressure correction (CPC) scheme

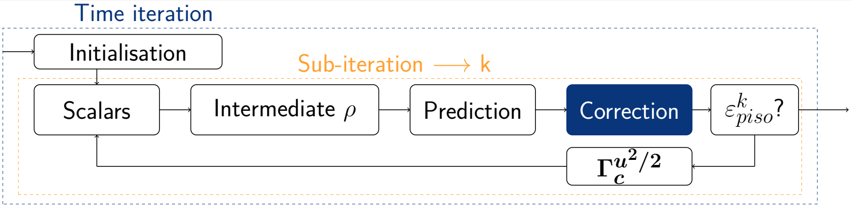

Features

- Variable time convergence order
- Total energy conservation
- ρ dependence on T
- EOS linearisation
- ρ dependence on p

Mass and simplified momentum equations solved between $[n; n+1, k]$

$$\begin{cases} \dfrac{\Theta\left(\rho_c^n,\, \rho_c^{n+1,k}\right) \underline{u}_c^{n+\theta,k} - \Theta\left(\rho_c^n,\, \rho_c^{n+1,k-1}\right) \widetilde{\underline{u}}_c^k}{\Delta t} + \underline{\nabla}_c \phi^k = 0, \\[2ex] \mathrm{Div}_c\left(\underline{q}_f\Big|_n^{n+1,k}\right) + \dfrac{\rho_c^{n+1,k} - \rho_c^n}{\Delta t} = 0, \end{cases}$$

$$\phi_c^k = \Theta\left(p_c\Big|_{n-2+\theta}^{n-1+\theta},\, p_c^{n+1,k}\right) - p_c\Big|_{n-1+\theta}^{n+\theta,k-1}.$$

$$\underline{q}_f\Big|_n^{n+1,k} = \left\langle \Theta\left(\rho^n,\, \rho^{n+1,k}\right) \underline{u}^{n+\theta,k} \right\rangle_f = \left\langle \Theta\left(\rho^n,\, \rho^{n+1,k-1}\right) \widetilde{\underline{u}}^k \right\rangle_f - \Delta t \underline{\nabla}_f \phi^k$$

Proposition : compressible pressure correction (CPC) scheme

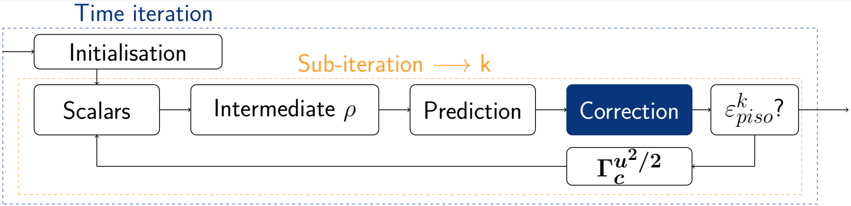

Features

- Variable time convergence order
- Total energy conservation
- ρ dependence on T
- EOS linearisation
- ρ dependence on p

Helmholtz equation for $p_c^{n+1,k}$:

$$\frac{1}{\Delta t}\left(\frac{\partial \rho}{\partial p}\right)_T (p_c^{n+1,k-1}, T_c^{n+1,k}) p_c^{n+1,k} - \theta \mathrm{Lapl}_c\left(\Delta t, p_c^{n+1,k}\right) = -\frac{(\widetilde{\rho}_c^k - \rho_c^n)}{\Delta t}$$
$$- \mathrm{Div}_c\left(\left\langle \Theta\left(\rho^n, \rho^{n+1,k-1}\right)\underline{\widetilde{u}}^k + \Delta t\left(\underline{\nabla} p|_{n-1+\theta}^{n+\theta,k-1} + \delta \underline{f}^k\right)\right\rangle_f\right) + (1-\theta)\mathrm{Lapl}_c\left(\Delta t, p|_{n-2+\theta}^{n-1+\theta}\right)$$

Proposition : compressible pressure correction (CPC) scheme

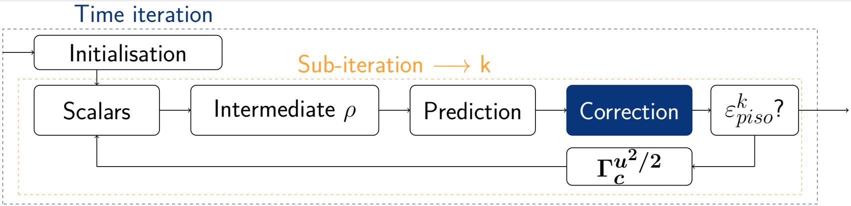

Features

- Variable time convergence order
- Total energy conservation
- ρ dependence on T
- EOS linearisation
- ρ dependence on p

Density update :

$$\boldsymbol{\rho_c^{n+1,k}} = \frac{p_c^{n+1,k}}{R_a T_c^{n+1,k}}$$

Velocity update :

$$\Theta\left(\rho_c^n,\ \rho_c^{n+1,k}\right) \boldsymbol{\underline{u}_c^{n+\theta,k}} = \Theta\left(\rho_c^n,\ \rho_c^{n+1,k-1}\right) \underline{\widetilde{u}}_c^k - \Delta t \underline{\nabla}_c \phi^k$$

Proposition : compressible pressure correction (CPC) scheme

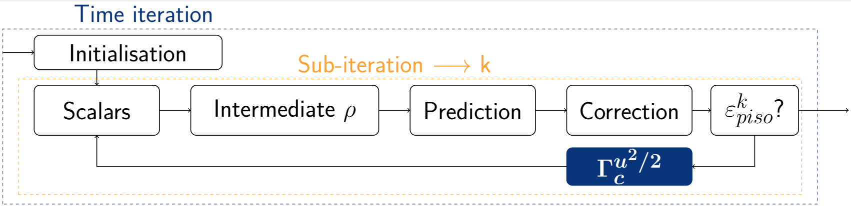

Features

- Variable time convergence order
- Total energy conservation
- ρ dependence on T EOS linearisation
- ρ dependence on p

Based on the discrete kinetic energy equation :

$$\frac{\Theta\left(\rho_c^n,\ \rho_c^{n+1,k}\right)|\underline{u}_c^{n+\theta,k}|^2-\Theta\left(\rho_c^{n-1},\ \rho_c^{n,k-1}\right)|\underline{u}_c^{n-1+\theta}|^2}{2\Delta t}+\mathrm{Div}_c\left(\frac{\left|\left\langle\Theta\left(\underline{u}^{n-1+\theta},\ \widetilde{\underline{u}}^k\right)\right\rangle_f\right|^2}{2}\left.\underline{q}_f\right|_{n-1+\theta}^{n+\theta,k-1}\right)$$

$$=-\Gamma_c^{u^2/2}\Big|_n^{n+1,k}+\overbrace{\Gamma_c^p|_n^{n+1}}^{\text{second order term}}-\underline{\mathrm{Grad}}_c\left(\left\langle p|_{n-1+\theta}^{n+\theta,k}\right\rangle_f\right)\cdot\underline{u}_c^{n+\theta,k}.$$

Adapted from Herbin et al, 2020, Eq. (e) + Eq. $\left(\frac{|u|^2}{2}\right) \longrightarrow$ Eq. (E_{tot})